Does Aspartate 170 of the D1 Polypeptide Ligate the Manganese Cluster in Photosystem II? An EPR and ESEEM Study†

Richard J. Debus,*,‡ Constantino Aznar,§ Kristy A. Campbell,§,|| Wolfgang Gregor,§ Bruce A. Diner,⊥ and R. David Britt*,§

Department of Biochemistry, University of California, Riverside, California 92521-0129, Department of Chemistry, University of California, Davis, California 95616, and Central Research and Development, Experimental Station, E. I. du Pont de Nemours & Company, Wilmington, Delaware 19880-0173

Received May 22, 2003; Revised Manuscript Received July 22, 2003

ABSTRACT: Aspartate 170 of the D1 polypeptide provides part of the high-affinity binding site for the first Mn(II) ion that is photooxidized during the light-driven assembly of the $(Mn)_4$ cluster in photosystem II [Campbell, K. A., Force, D. A., Nixon, P. J., Dole, F., Diner, B. A., and Britt, R. D. (2000) *J. Am. Chem. Soc. 122*, 3754−3761]. However, despite a wealth of data on D1-Asp170 mutants accumulated over the past decade, there is no consensus about whether this residue ligates the assembled $(Mn)_4$ cluster. To address this issue, we have conducted an EPR and ESEEM (electron spin-echo envelope modulation) study of D1-D170H PSII particles purified from the cyanobacterium *Synechocystis* sp. PCC 6803. The line shapes of the S_1 and S_2 state multiline EPR signals of D1-D170H PSII particles are unchanged from those of wild-type PSII particles, and the signal amplitudes correlate approximately with the lower O_2 evolving activity of the mutant PSII particles (40−60% compared to that of the wild type). These data provide further evidence that the assembled $(Mn)_4$ clusters in D1-D170H cells function normally, even though the assembly of the $(Mn)_4$ cluster is inefficient in this mutant. In the two-pulse frequency domain ESEEM spectrum of the 9.2 GHz S_2 state multiline EPR signal of D1-D170H PSII particles, the histidyl nitrogen modulation observed at 4−5 MHz is unchanged from that of wild-type PSII particles and no significant new modulation is observed. Three scenarios are presented to explain this result. (1) D1-Asp170 ligates the assembled $(Mn)_4$ cluster, but the hyperfine couplings to the ligating histidyl nitrogen of D1-His170 are too large or anisotropic to be detected by ESEEM analyses conducted at 9.2 GHz. (2) D1-Asp170 ligates the assembled $(Mn)_4$ cluster, but D1-His170 does not. (3) D1-Asp170 does not ligate the assembled $(Mn)_4$ cluster.

The catalytic site of water oxidation in photosystem II (PSII)[1] contains a cluster of four Mn ions and the redox-active tyrosine residue known as Y_Z (for reviews, see refs *1*−*9*). One Ca ion and one Cl ion are required for catalytic activity and appear to be located in the vicinity of the $(Mn)_4$ cluster. The $(Mn)_4$ cluster accumulates oxidizing equivalents in response to light-induced electron transfer reactions within PSII, thereby providing the interface between one-electron photochemistry and the four-electron process of water oxidation. Tyrosine Y_Z serves as the immediate oxidant of the $(Mn)_4$ cluster, transferring an electron from the $(Mn)_4$ cluster to $P_{680}^{+\bullet}$ in response to the light-induced formation of the latter. During each catalytic cycle, the $(Mn)_4$ cluster cycles through five oxidation states termed S_n, where n denotes the number of oxidizing equivalents stored. The S_1 state predominates in dark-adapted samples. Most interpretations of XANES data have concluded that the S_1 state consists of two Mn(III) and two Mn(IV) ions and that the S_2 state consists of one Mn(III) and three Mn(IV) ions (*2*, *3*, *10*−*12*), but an alternative view exists (*13*, *14*). The additional oxidizing equivalent of the S_3 state may be localized on an Mn ligand (refs *12* and *15*, but see ref *11*). The S_4 state is a transient intermediate (possibly corresponding to the $Y_Z^{\bullet}S_3$ state) that reverts to the S_0 state with the concomitant release of O_2.

The electron density of the Mn cluster is visible in the recent 3.6−3.8 Å structures of PSII (*16*−*18*), but the exact arrangement of the Mn ions is unknown. The resolutions of

† This work was supported by the National Institutes of Health (Grant GM66136 to R.J.D. and Grant GM48242 to R.D.B.).

* To whom correspondence should be addressed. R.J.D.: phone, (909) 787-3483; fax, (909) 787-4434; e-mail, richard.debus@ucr.edu. R.D.B.: phone, (530) 752-6377; fax, (530) 752-8995; e-mail, rdbritt@ucdavis.edu.

‡ University of California, Riverside.

§ University of California, Davis.

|| Present address: Micron Technology, Inc., 8000 South Federal Way, Boise, ID 83707-0006.

⊥ E. I. du Pont de Nemours & Co.

[1] Abbreviations: Chl, chlorophyll; DCMU, 3-(3,4-dichlorophenyl)-1,1-dimethylurea; DMSO, dimethyl sulfoxide; ENDOR, electron nuclear double resonance; EPR, electron paramagnetic resonance; ESE, electron spin-echo; ESEEM, electron spin-echo envelope modulation; EXAFS, extended X-ray absorption fine structure; MES, 2-(*N*-morpholino)-ethanesulfonic acid; NTA, nitrilotriacetic acid; P_{680}, chlorophyll species that serves as the light-induced electron donor in PSII; Pheo, pheophytin; PSII, photosystem II; Q_A, primary plastoquinone electron acceptor; TES, *N*-[tris(hydroxymethyl)methyl]-2-aminoethanesulfonic acid; wild-type*, control strain of *Synechocystis* sp. strain PCC 6803 constructed in a fashion identical to that of the D1-D170H mutant, but containing the wild-type *psb*A-2 gene; Y_Z, tyrosine residue that mediates electron transfer between the Mn cluster and $P_{680}^{+\bullet}$; XANES, X-ray absorption near edge structure.

10.1021/bi034859f CCC: $25.00
Published on Web 08/21/2003

the current X-ray structures are not sufficient to provide this information. Nevertheless, EXAFS studies have detected the presence of two to three Mn−Mn interactions with distances of ∼2.7 Å and at least one Mn−Mn and/or Mn−Ca interaction with a distance of ∼3.3 Å (*2*, *3*, *10*−*12*). These distances, along with recent simulations of EPR and ENDOR data of samples poised in the S_2 state, have provided families of possible arrangements for the $(Mn)_4$ cluster, predicting it to be a strongly exchange-coupled trimer that is weakly exchange-coupled to a fourth Mn ion (*19*, *20*). These arrangements are compatible with the recent 3.6−3.8 Å X-ray structures.

On the basis of numerous mutational and biochemical studies, most or all of the amino acid residues that ligate the $(Mn)_4$ cluster are expected to be contributed by the D1 protein (for reviews, see refs *4*, *21*, and *22*). While the recent 3.6−3.8 Å structures are consistent with this expectation (*16*−*18*), the resolutions of these structures are insufficient for identifying the individual protein ligands. Many mutational studies have targeted D1-Asp170 as a possible ligand of the $(Mn)_4$ cluster, and at least 18 mutations have been constructed at this position: D170E, D170Q, D170N, D170H, D170C, D170M, D170S, D170T, D170A, D170G, D170V, D170L, D170I, D170R, D170Y, D170F, D170W, and D170P (*23*−*28*). The D170E mutant is photoautotrophic and evolves O_2 at ∼60% of the rate of wild-type cells. The D170H and D170V mutants are weakly photoautotrophic and evolve O_2 at ∼50 and ∼40% of the rate of wild-type cells, respectively. Photoautotrophic growth is abolished in all other mutants. Among the non-photoautotrophic mutants, O_2 evolution is abolished in D170S, D170T, D170A, D170G, D170Y, and D170P cells, nearly abolished in D170N and D170W cells, and diminished substantially in all others. In those mutants that evolve O_2, the assembled $(Mn)_4$ clusters appear to behave normally, exhibiting O_2 flash yields with normal period 4 oscillations and exhibiting normal or slightly decreased S_2/S_1 midpoint potentials (*23*−*28*). In the O_2-evolving mutants, significant fractions of PSII reaction centers lack $(Mn)_4$ clusters *in vivo*: this fraction is 20−25% in the D170E mutant, ∼50% in the D170H and D170V mutants, and ∼60% in the D170L, D170I, and D170R mutants (*26*, *28*). In these mutants, the $(Mn)_4$ cluster has been proposed to be unstable or to be assembled inefficiently (*23*−*28*).

The high-affinity Mn(II) binding site on the apoprotein is abolished in at least the D170N, D170A, and D170S mutants (*23*, *24*). When Mn-depleted wild-type PSII particles are illuminated in the presence of Mn(II) ions, $Y_Z^{\bullet}$ oxidizes Mn(II) to Mn(III) and a parallel polarization EPR signal of the Mn(III) ion is observed (*29*). In Mn-depleted D170E and D170H PSII particles, $Y_Z^{\bullet}$ is also capable of oxidizing Mn(II) ions (*23*, *24*, *29*). However, a different Mn(III) EPR signal is observed in D170H PSII particles, and no Mn(III) EPR signal is observed in D170E PSII particles (*29*). Instead, the illuminated D170E PSII particles exhibit a perpendicular polarization EPR signal suggestive of Mn(IV) (*29*). These results show that D1-Asp170 forms part of the binding site for the first Mn(II) ion that is photooxidized during the light-driven assembly (photoactivation) of the Mn cluster and that the residue that is present at this position influences the coordination environment and redox properties of the photooxidized Mn(II) ion.

If D1-Asp170 ligates the first Mn(II) ion that is photooxidized during photoactivation of the Mn cluster, it would seem logical that this residue would also ligate the assembled $(Mn)_4$ cluster. Indeed, most studies of D1-Asp170 mutants have suggested this possibility (*23*−*28*). In one such study, conducted with D1-D170H PSII particles purified from the unicellular cyanobacterium *Synechocystis* sp. PCC 6803, low-frequency FTIR difference spectroscopy was employed to show that D1-Asp170 is structurally coupled to an Mn−O−Mn unit having a vibrational mode that shifts from ∼625 to ∼606 cm^{-1} during the $S_1 \rightarrow S_2$ transition (*30*). This coupling implies that D1-Asp170 either ligates the $(Mn)_4$ cluster directly or participates in one or more hydrogen bonds to the $(Mn)_4$ cluster (*30*). However, no study has provided definitive proof that D1-Asp170 ligates the assembled $(Mn)_4$ cluster. Indeed, one could argue that D1-Asp170 is unlikely to ligate the assembled $(Mn)_4$ cluster because D1-D170V cells are weakly photoautotrophic and D1-D170L and D1-D170I cells evolve O_2 at ∼20% of the rate of wild-type* cells (*28*); neither Val, Leu, nor Ile would be expected to ligate Mn.

In this study, we present a 9 GHz EPR and ESEEM analysis of *Synechocystis* D1-D170H PSII particles to further characterize the nature of the $(Mn)_4$ clusters in this mutant and to further address whether D1-Asp170 ligates the assembled $(Mn)_4$ cluster. The pulsed EPR method of ESEEM spectroscopy is a powerful tool for detecting weak hyperfine couplings in paramagnetic systems (*31*−*35*). We recently showed that D1-His332 almost certainly ligates the $(Mn)_4$ cluster in PSII on the basis of a 9.2 GHz ESEEM study of *Synechocystis* D1-H332E PSII particles (*36*). In D1-H332E PSII particles, the 4−5 MHz histidyl nitrogen feature that is observed in the two-pulse frequency domain ESEEM spectrum of the 9.2 GHz S_2 state multiline EPR signal in wild-type* PSII particles was sharply diminished, consistent with direct ligation of the $(Mn)_4$ cluster by D1-His332. Therefore, if D1-Asp170 ligates the $(Mn)_4$ cluster and the ligating carboxylate oxygen is replaced with a histidyl nitrogen in the D1-D170H mutant, the hyperfine coupling between the ligating nitrogen atom of His170 and the unpaired electron spin on the ligated Mn ion should be able to be detected by ESEEM spectroscopy, provided that the hyperfine coupling is sufficiently weak and is not extremely anisotropic. If these conditions are satisfied, the additional nitrogen coupling should be manifested either as an increase in the amplitude of the 4−5 MHz histidyl nitrogen feature in the two-pulse frequency domain ESEEM spectrum of the 9.2 GHz S_2 state multiline EPR signal, as a broadening of this feature, or as additional nitrogen modulation at a different frequency.

MATERIALS AND METHODS

Construction of the Site-Directed Mutant. The constructions of the D1-D170H mutant and wild-type* control strains of cyanobacterium *Synechocystis* sp. strain PCC 6803 were described previously (*30*). Briefly, the D1-D170H mutation was constructed in the *psbA-2* gene (*26*), and the mutation-bearing plasmid was transformed into a host strain of *Synechocystis* that lacks all three *psbA* genes (*37*) and contains a His tag on the carboxy terminus of CP47 (*36*). Single colonies were selected for their ability to grow on solid media containing 5 μg/mL kanamycin monosulfate (*37*). The control wild-type* strain (*30*) was constructed in an

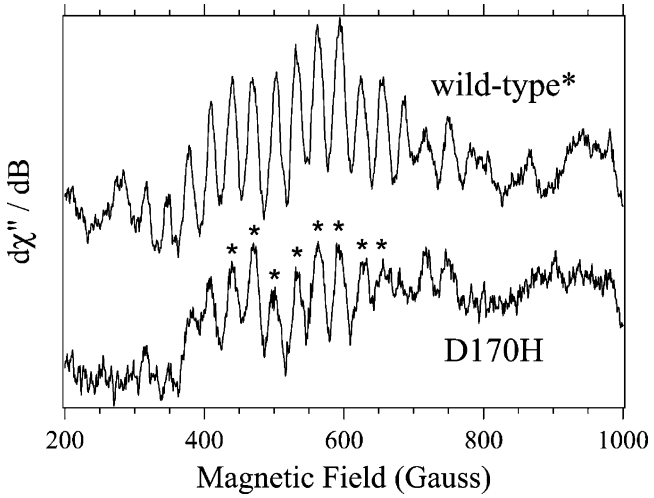

FIGURE 1: Parallel polarization S_1 state multiline EPR signal of dark-adapted *Synechocystis* wild-type* (top trace) and D1-D170H (bottom trace) PSII particles. Samples contained approximately 7 mg of Chl/mL in 25% (v/v) glycerol, 50 mM MES-NaOH (pH 6.0), 20 mM $CaCl_2$, 5 mM $MgCl_2$, 0.03% (w/v) *n*-dodecyl β-D-maltoside, 1 mM DCMU, and 1% (v/v) DMSO. Samples were deaerated prior to measurement to remove dissolved O_2. Experimental conditions were as follows: dual-mode cavity, microwave frequency of 9.43 GHz, microwave power of 50 mW, modulation amplitude of 8 G, modulation frequency of 100 kHz, time constant of 164 ms, conversion time of 164 ms, and temperature of 2.7 K. Each spectrum represents the accumulation of 30 scans.

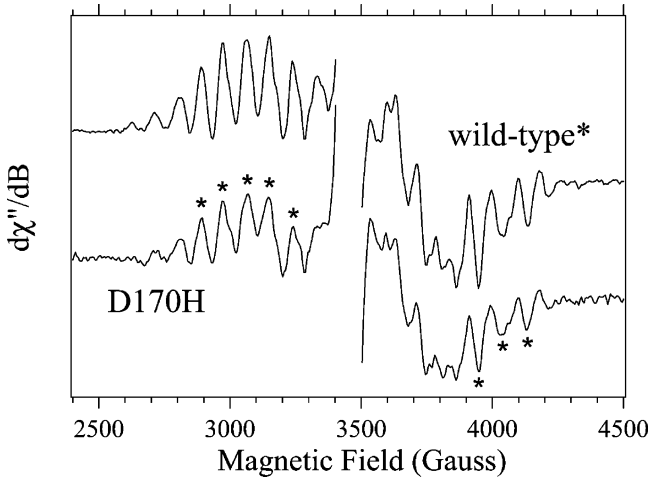

FIGURE 2: Light-*minus*-dark perpendicular polarization S_2 state multiline EPR signal of *Synechocystis* wild-type* (top trace) and D1-D170H (bottom trace) PSII particles. Both spectra have had the large $g = 2$ signal of $Y_D^{\bullet}$ excised for clarity. Samples were illuminated for 5 min at 195 K before being flash-frozen in liquid N_2. Samples contained approximately 4 mg of Chl/mL in 25% (v/v) glycerol, 50 mM MES-NaOH (pH 6.0), 20 mM $CaCl_2$, 5 mM $MgCl_2$, 0.03% (w/v) *n*-dodecyl β-D-maltoside, 1 mM DCMU, and 1% (v/v) DMSO. Experimental conditions were as follows: dual-mode cavity, microwave frequency of 9.69 GHz, microwave power of 5 mW, modulation amplitude of 10 G, modulation frequency of 100 kHz, time constant of 41 ms, conversion time of 82 ms, and temperature of 7 K. The wild-type* and D1-D170H spectra represent the accumulations of 50 and 60 scans, respectively.

identical fashion except that the transforming plasmid carried no site-directed mutation. The designation wild type* differentiates this strain from the native wild-type strain that contains all three *psb*A genes and is sensitive to antibiotics.

Propagation of Cultures. The wild-type* and D1-D170H cells were maintained on solid BG-11 medium (*38*) containing 5 mM TES-NaOH (pH 8.0), 0.3% (w/v) sodium thiosulfate, 5 mM glucose, 10 μM DCMU, and 5 μg/mL kanamycin monosulfate, as described previously (*26*). The DCMU, kanamycin monosulfate, and sodium thiosulfate were omitted from liquid cultures. For the isolation of PSII particles, cells were grown in modified 250 mL Erlenmeyer flasks as described previously (*26*) until they reached an optical density of 0.9−1.2 at 730 nm. Cells were then transferred to two 20 L carboys, each containing 15 L of growth medium, and grown as described previously (*39*) until their optical densities reached 0.9−1.2 at 730 nm (typically 4 days for wild-type* and 4−5 days for D1-D170H cultures). Optical densities were measured with a modified CARY 14 spectrophotometer (OLIS, Inc., Bogart, GA).

Purification of PSII Particles. For the experiments whose results are depicted in Figure 1, PSII particles were purified under dim green light with Ni−NTA superflow affinity resin (Qiagen) as described previously (*30*, *36*). For all other experiments, this purification procedure was modified as follows: the *n*-dodecyl β-D-maltoside-extracted thylakoid membranes were centrifuged for 10 min at 24000*g* (we thank G. W. Brudvig and co-workers for this suggestion), the supernatant was diluted with an equal volume of column buffer [50 mM MES-NaOH (pH 6.0), 20 mM $CaCl_2$, 5 mM $MgCl_2$, 0.03% (w/v) *n*-dodecyl β-D-maltoside, and 25% (w/v) glycerol] to decrease the concentration of *n*-dodecyl β-D-maltoside approximately 2-fold, and the diluted supernatant was pumped directly onto the 40 mL, 5 cm diameter, Ni−NTA superflow affinity resin column at 3 mL/min. The purified PSII particles were eluted in 7−8 column volumes with column buffer containing 50 mM L-histidine. The eluent was brought to 1 mM EDTA, concentrated by ultrafiltration (Amicon models 2000 and 8400 fitted with YM-100 membranes) to a volume of 5−10 mL, brought to 6 mM EDTA, passed through a G-25 column to remove histidine, EDTA, and EDTA-complexed metal ions, then concentrated to 1−2 mg of Chl/mL (Amicon models 8050 and 8010 fitted with YM-100 membranes), frozen in liquid N_2, and stored at −80 °C. Shortly before the EPR and ESEEM experiments, the PSII particles were further concentrated to 4−7 mg of Chl/mL with Centricon-100 concentrators (Millipore Corp., Bedford, MA). The concentrated samples were then mixed with DCMU dissolved in DMSO [to 1 mM DCMU and 1% (v/v) DMSO], loaded into 3.8 mm (outside diameter) precision quartz EPR tubes, dark-adapted on ice for 20 min, and then frozen in liquid N_2 [the DCMU was added to permit formation of the S_2 state by illumination at elevated temperatures if needed (*36*, *40*), although ultimately all samples were illuminated at 195 K only]. The light-saturated rates of evolution of O_2 from the purified wild-type* and D1-D170H PSII particles were 3.1−3.2 and 1.2−1.9 mmol of O_2 (mg of Chl)$^{-1}$ h^{-1}, respectively.

EPR, ESE, and ESEEM Measurements. Continuous-wave EPR spectra were recorded with a Bruker ECS106 X-band CW-EPR spectrometer equipped with an ER-4116DM dual-mode cavity. Cryogenic temperatures were obtained with an Oxford ESR900 liquid helium cryostat. The temperature was controlled with an Oxford ITC503 temperature and gas flow controller that was equipped with a gold−iron chromel thermocouple. Signal amplitudes were estimated from the integrated areas of selected peaks (marked with asterisks in Figures 1 and 2) after baseline subtraction between the points

delimiting each peak. Field-swept two-pulse ESE spectra and two-pulse ESEEM spectra were recorded with a laboratory-built pulsed 8−18 GHz EPR spectrometer (*41*). For the parallel mode EPR studies, condensed air was purged from the EPR tubes by warming the tubes to 198 K (in dry ice and methanol) and directing a stream of Ar gas over the sample for 2 min followed by rapid refreezing in liquid N_2. This treatment was found to minimize the large background signals that are often observed in parallel mode spectra of PSII (e.g., refs *42*−*44*). For the perpendicular mode EPR and ESEEM studies, the S_2 state was generated by illuminating samples for 5 min in a nonsilvered dewar at 198 K (dry ice and methanol) with a focused 300 W IR-filtered Radiac light source and a Schott 150 W IR-filtered fiber optic lamp. The samples were then immediately frozen in liquid nitrogen. For each sample, both the background field-swept two-pulse ESE spectrum and the background two-pulse time domain ESEEM patterns were obtained before the sample was illuminated. To isolate the ESEEM patterns of the S_2 state multiline EPR signal, the ESEEM patterns obtained prior to illumination were subtracted from the ESEEM patterns obtained after illumination. The light-*minus*-dark ESEEM patterns were normalized to their first maxima so that the calculated frequency domain ESEEM spectra would correspond to normalized multiline signal intensities. Frequency domain ESEEM spectra were obtained by calculating the cosine Fourier transforms of the normalized light-*minus*-dark two-pulse time domain data after reconstruction of the instrumental dead times with the Fourier backfill method described by Mims (*45*). The frequencies used for Fourier backfilling are included in the legend of Figure 5. The same relative amplitudes were used for each class of backfilled frequency components to allow for a nonbiased quantitative comparison of the final Fourier transforms.

Other Procedures. Chlorophyll concentrations and light-saturated rates of O_2 evolution were measured as described previously (*26*, *39*).

RESULTS

Continuous-Wave EPR Spectra. A parallel polarization, integer spin multiline EPR signal was observed in dark-adapted *Synechocystis* D1-D170H PSII particles (Figure 1, bottom trace). In terms of peak positions and splittings, this signal resembles the S_1 state multiline EPR signal that is observed in *Synechocystis* wild-type* PSII particles (Figure 1, top trace) (*42*−*44*), and we assign it to the S_1 state in D1-D170H PSII particles. The integrated area of the eight indicated peaks in the D1-D170H spectrum was approximately 66% of the integrated area of the eight corresponding peaks in the wild-type* spectrum. The lower signal amplitude in the D1-D170H PSII particles correlated approximately with the lower O_2 evolving activity of the D1-D170H preparations (40−60% compared to that of wild type*).

A perpendicular polarization multiline EPR signal was observed in D1-D170H PSII particles after illumination at 195 K (Figure 2, bottom trace). In terms of peak positions and splittings, this signal resembles the S_2 state multiline EPR signal observed in wild-type* PSII particles illuminated under the same conditions (Figure 2, top trace), and we assign it to the S_2 state in D1-D170H PSII particles. After we had corrected for the different numbers of scans that accumulated, the integrated area of the eight indicated peaks in the D1-D170H spectrum was approximately 52% of the integrated area of the eight corresponding peaks in the wild-type* spectrum. The lower signal amplitude also correlated approximately with the lower O_2 evolving activity of the D1-D170H PSII preparations. A normal S_2 state multiline EPR signal was also observed in D1-D170H PSII particles purified with conventional DEAE chromatography (as in ref *46*) (not shown).

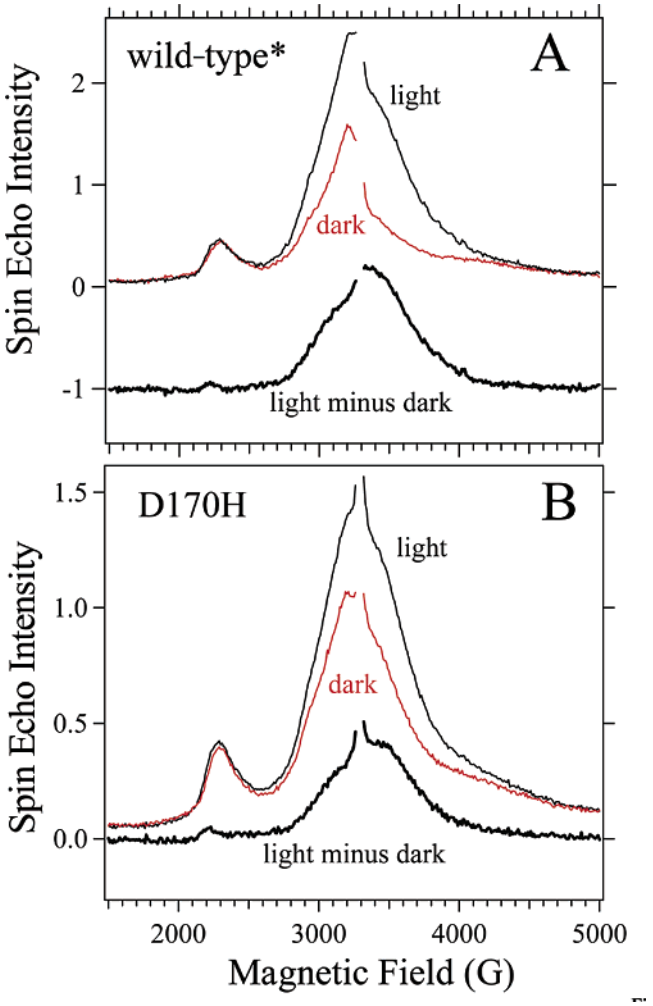

FIGURE 3: ESE field-swept EPR spectra of (A) wild-type* and (B) D1-D170H PSII particles. Each panel shows the ESE field-swept EPR spectrum of the sample prior to illumination (middle traces, red lines), the ESE field-swept EPR spectrum of the sample after illumination (top traces, thin black lines), and the light-*minus*-dark difference spectrum (bottom traces, bold black lines). The large $g = 2$ signals of $Y_D^{\bullet}$ have been excised, and the light-*minus*-dark difference spectrum of the wild type* has been offset for clarity. Samples were illuminated for 5 min at 195 K before being flash-frozen in liquid N_2. Samples contained approximately 6 mg of Chl/mL in 25% (v/v) glycerol, 50 mM MES-NaOH (pH 6.0), 20 mM $CaCl_2$, 5 mM $MgCl_2$, 0.03% (w/v) *n*-dodecyl β-D-maltoside, 1 mM DCMU, and 1% (v/v) DMSO. Experimental conditions were as follows: microwave frequency of 9.229 GHz, microwave pulse peak power of 25 W, $\pi/2$ pulse width of 15 ns, π pulse width of 25 ns, τ of 210 ns, repetition time of 5 ms, and temperature of 4.2 K.

ESE Field-Swept EPR Spectra. The ESE field-swept EPR spectra of *Synechocystis* wild-type* and D1-170H PSII particles are compared in Figure 3. The spectra resemble each other and are similar to ESE field-swept EPR spectra of *Synechocystis* wild-type PSII particles reported previously

(*36*, *47*). On a chlorophyll basis, the background signal is larger in dark-adapted wild-type* PSII particles than in dark-adapted D1-D170H PSII particles (the reason for the larger background signal in wild type* is not known), but the peak near 2300 G has a similar amplitude in both samples. This peak corresponds to the g_z turning point of the oxidized form of cytochrome b_{559}. Illumination of some D1-D170H PSII preparations caused a significant increase in the amplitude of this peak, evidence of an apparent photooxidation of this cytochrome. The EPR signal of the oxidized form of cytochrome b_{559} underlies much of the S_2 state multiline EPR signal [$g_z \approx 3.0$, $g_y \approx 2.2$, and $g_x \approx 1.5$ for cytochrome b_{559} in *Synechocystis* sp. strain PCC 6803 (*48*)]. Therefore, any photooxidation of cytochrome b_{559} could contaminate the S_2 state ESEEM spectra with subtraction artifacts from the cytochrome heme and histidyl ligand nitrogens. Consequently, samples were screened, and only those exhibiting negligible cytochrome b_{559} photooxidation (three samples of five that were examined) were included in our analysis of histidyl ligation in the D1-D170H mutant. We have noted previously that variable fractions of mutant PSII preparations from *Synechocystis* sp. PCC 6803 exhibit light-induced cytochrome b_{559} redox changes (*36*).

The light-*minus*-dark ESE field-swept EPR spectra of the S_2 state multiline signal in wild-type* and D1-D170H PSII particles closely resembled each other in terms of width and overall line shape (Figure 3). The integrated areas of the signals in the mutant PSII preparations that exhibited negligible cytochrome b_{559} photooxidation were 40−50% of those in the wild-type* preparations on a chlorophyll basis, again correlating approximately with the lower O_2 evolving activity of the D1-D170H PSII preparations.

ESEEM Spectra. Two-pulse time domain ESEEM patterns recorded at the magnetic field position (3417 G) where the light-*minus*-dark ESE field-swept EPR spectra were near maximal are shown in Figure 4 for wild-type* and D1-D170H PSII particles. To eliminate all modulations other than those arising from magnetic nuclei coupled to the S_2 state of the Mn cluster, the background ESEEM patterns were subtracted from the light-induced ESEEM patterns to yield the light-*minus*-dark ESEEM patterns shown with thick black lines. Frequency domain ESEEM spectra were calculated from the normalized light-*minus*-dark time domain patterns after reconstruction of the instrumental dead times (Figure 5). In Figure 5, the frequency domain ESEEM spectra of three separate D1-D170H PSII preparations (#1−#3, black lines) are shown overlaid with the spectrum of wild-type* PSII particles (red lines). To facilitate comparison of D1-D170H and wild-type* spectra, the bottom traces of Figure 5 show the average of the three separate D1-D170H frequency domain spectra overlaid with the wild-type* spectrum after renormalization of the spectra to the transform amplitudes at 14.5 MHz.

In the frequency domain ESEEM spectrum of wild-type* PSII particles, the peak at 4−5 MHz corresponds to nitrogen modulation from one or more Mn histidyl ligands (*36*, *47*, *49*). The broad feature at 8−9 MHz cannot be reproduced in all wild-type* spectra (not shown) and may be an artifact. The peak at 14−15 MHz corresponds to protons that are weakly coupled to the electron spin of the Mn cluster and that are resonating at or near the proton Larmor frequency (*50*). These protons also give rise to the negative "sum" peak

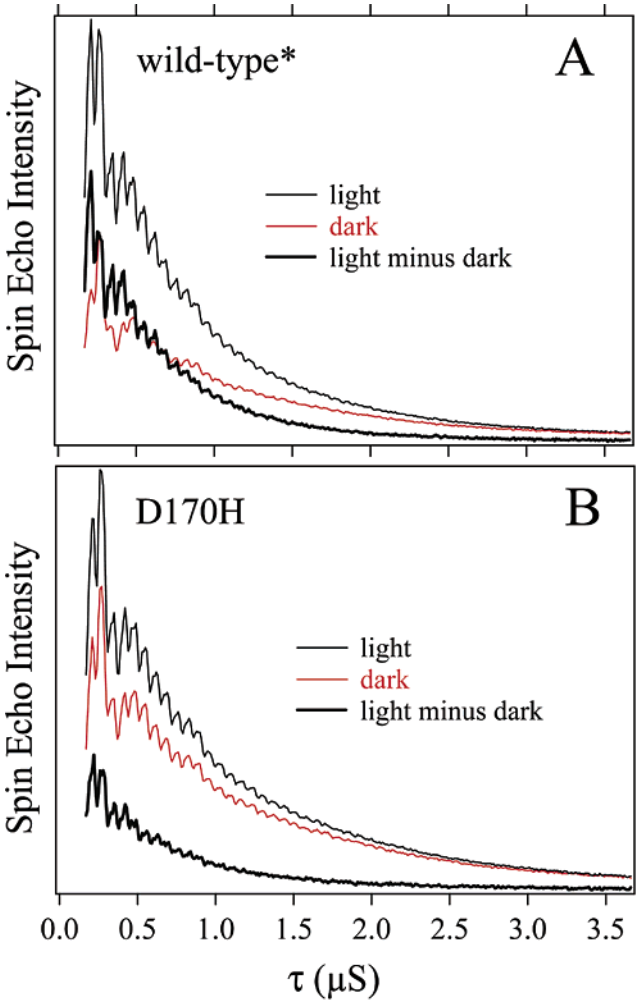

FIGURE 4: Two-pulse time domain ESEEM patterns of (A) wild-type* and (B) D1-D170H PSII particles. Shown are the ESEEM patterns of the samples prior to illumination (red lines), the ESEEM patterns after illumination (thin black lines), and their difference (thick black lines), corresponding to the ESEEM patterns of the light-induced S_2 state of the Mn cluster. The samples were those used in Figure 3. Experimental conditions were as follows: magnetic field of 3417 G, microwave frequency of 9.229 GHz, microwave pulse peak power of 25 W, $\pi/2$ pulse width of 15 ns, π pulse width of 25 ns, repetition time of 5 ms, and temperature of 4.2 K. The interval, τ, between pulses in the two-pulse sequence was increased from 170 to 3670 ns in 10 ns increments.

that is centered near 29 MHz, at approximately twice the proton Larmor frequency.[2]

In all D1-D170H PSII preparations exhibiting negligible photooxidation of cytochrome b_{559}, the amplitude of the nitrogen modulation at 4−5 MHz was similar to that in wild-type* PSII preparations and no significant new modulation was evident. The slight shifts toward lower frequency of the feature at 8−9 MHz and of the histidyl nitrogen modulation at 4−5 MHz may be caused by a slight alteration of the coupling between the electron spin of the $(Mn)_4$ cluster and the native histidyl ligand(s) (e.g., D1-His332) that is caused by subtle structural rearrangements associated with changing D1-Asp170 to His. The coupling energies are so small (≤1

[2] Density matrix analysis shows that, in addition to the fundamental nuclear spin transition frequencies, the sum and difference of these frequencies also appear in two-pulse ESEEM spectra; their negative phases result in inverted peaks in the cosine Fourier transform (*51*−*53*).

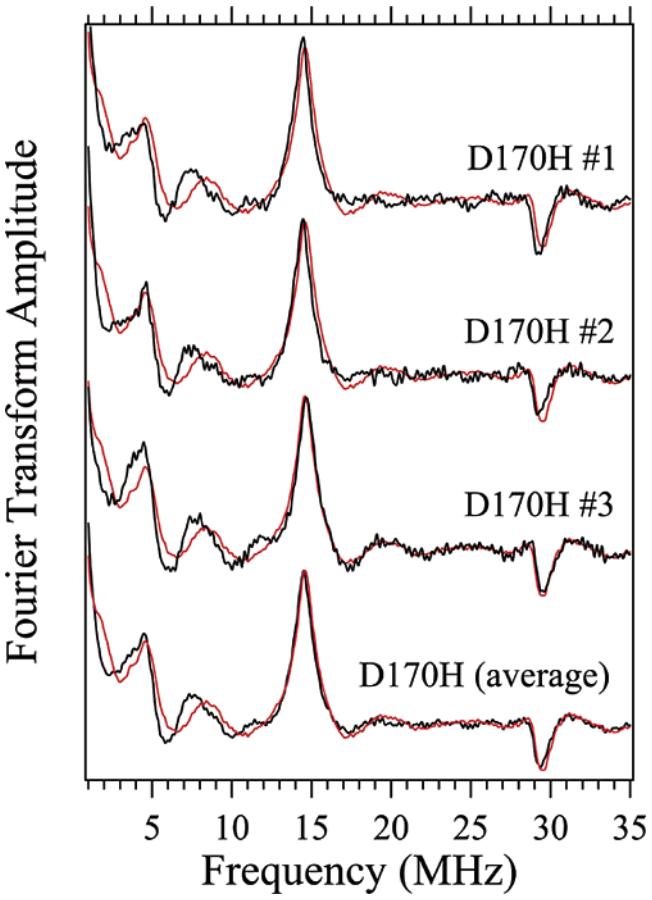

FIGURE 5: Cosine Fourier transforms of normalized two-pulse time domain light-*minus*-dark ESEEM patterns of three independent preparations of D1-D170H PSII particles (preparations #1−#3, black lines) and one wild-type* preparation (red line in each set) calculated after reconstruction of the instrumental dead times (0−170 ns). Preparation D170H #1 corresponds to the sample shown in Figures 3 and 4. The spectra have *not* been renormalized. The bottom pair of transforms shows the average of all three D170H cosine Fourier transforms (black line) compared to the wild-type* transform (red line) after renormalization of the transform amplitudes at 14.5 MHz. Experimental conditions were the same as those given in the legend of Figure 4. Relative amplitudes of frequency components (0.3 MHz width each) used in Fourier backfilling to reconstruct the instrumental dead times: 3 (nitrogen peak at 4.4 MHz), 20 (proton peak at 14.5 MHz), and 10 (proton "sum peak" at 29.4 MHz).

MHz) that they would not be detected by conventional cw-EPR spectroscopy (Figures 1 and 2). Alternatively, these slight shifts might be caused by residual cytochrome b_{559} photooxidation in the D170H samples [note the very small light-induced increase in the g_z peak of oxidized cytochrome b_{559} at ∼2300 G in Figure 3B; cytochrome b_{559} exhibits ESEEM peaks near 4, 7.2, and 11.4 MHz (*54*, *55*)].

DISCUSSION

The light-saturated O_2 evolution rates of the D1-D170H PSII particles examined in this study were 40−60% of those of wild-type* PSII particles, in agreement with a previous study (*30*). These relative rates were similar to those of D1-D170H and wild-type cells (*23*, *26*, *27*), implying that the $(Mn)_4$ clusters found in D1-D170H cells are stable. The apparent correlation between the O_2 evolving activity of D1-D170H PSII particles and the integrated areas of the S_1 and S_2 state multiline EPR signals (shown in Figures 1 and 2, the latter also detected as an ESE field-swept spectrum, as shown in Figure 3) supports the conclusion of earlier studies (*23*, *26*, *27*) that significant fractions of D1-D170H PSII reaction centers lack $(Mn)_4$ clusters *in vivo*. The apparent stability of the assembled $(Mn)_4$ clusters in D1-D170H PSII particles implies that inefficient assembly of the $(Mn)_4$ cluster, not instability, is the reason that fewer $(Mn)_4$ clusters are assembled in D1-D170H cells. This explanation was originally proposed by P. J. Nixon and B. A. Diner (*23*, *24*).

We have shown that the S_1 state multiline EPR signal, the S_2 state multiline EPR signal, and the two-pulse frequency domain ESEEM spectrum of the S_2 state multiline EPR signal of D1-D170H PSII particles all resemble those of wild-type* PSII particles. These similarities support the conclusion of earlier studies (*23*, *26*, *27*) that those $(Mn)_4$ clusters that are assembled in D1-D170H cells function normally. These similarities also provide additional evidence that the D1-D170H mutation has not introduced unintended, secondary structural changes into the protein (*30*).

The presence of an additional histidyl nitrogen ligand in D1-D70H PSII particles would be difficult to detect with conventional EPR spectroscopy; even an additional histidyl nitrogen ligand having a strong hyperfine coupling of $A \approx$ 10 MHz (see below) would produce splittings of only ∼3 G. However, the presence of an additional nitrogen ligand should be detected with ESEEM spectroscopy if the hyperfine coupling is sufficiently weak and is not extremely anisotropic. To explain the similarity of the ESEEM spectra of the D1-D170H and wild-type* PSII preparations, we consider three possible scenarios.

Scenario 1. Both D1-Asp170 and D1-His170 Ligate the $(Mn)_4$ Cluster. This scenario requires that the additional hyperfine coupling between the ligating D1-His170 nitrogen atom and the $(Mn)_4$ cluster in D1-D170H PSII particles not be detected with ESEEM spectroscopy conducted at 9.2 GHz. There is ample precedent for a ligating nitrogen escaping detection by ESEEM spectroscopy; the hyperfine coupling need only be too strong or too anisotropic. For example, in Cu(II)−imidazole model compounds and in Cu(II) enzymes containing histidine bound equatorially to Cu(II), the hyperfine coupling to the directly coordinated nitrogen is approximately ∼40 MHz (*56*−*58*), easily observed with ENDOR spectroscopy (*56*−*58*) but too large to produce envelope modulation. In these Cu(II)−imidazole/histidine systems, only the hyperfine coupling to the remote nitrogen [1.5−1.8 MHz (*59*−*61*)] can be observed with ESEEM analyses[3] (*59*−*63*).

Additional examples of directly coordinated nitrogen atoms escaping detection by ESEEM spectroscopy are provided by model compounds and catalase enzymes containing di-μ_2-oxo-bridged Mn(III)Mn(IV) structures. These structures are components of several current models for the arrangement of the four Mn ions in PSII (*14*, *19*, *20*, *67*). In the Mn(III)-Mn(IV) model compounds, nitrogen atoms bound axially to

[3] In Mn(II)−imidazole model compounds and in Mn(II) enzymes containing histidine ligands, the hyperfine couplings are much weaker than in corresponding Cu(II) compounds and Cu(II) enzymes because the covalency of the metal−ligand interaction is lower. In Mn(II) enzymes, directly coordinated histidyl nitrogens have been detected with ESEEM spectroscopy, but remote histidyl nitrogens have not (*64*−*66*).

the Mn(III) ion have strong hyperfine couplings of 10−12 MHz (*68*−*70*). These couplings have been detected with ENDOR spectroscopy (*68*−*70*) but not with ESEEM spectroscopy [conducted at 11 GHz (*70*)]. The large couplings of the axially bound nitrogens arise because these nitrogens overlap the unpaired electron spin density that is concentrated by the Jahn−Teller effect in the d_z^2 orbital of the Mn(III) ion. Nitrogen atoms bound equatorially to the Mn(III) ion can also be difficult to detect (even with ENDOR spectroscopy) because the hyperfine interaction can be extremely anisotropic, spreading the spectral intensity over a large frequency range (*70*). On the other hand, nitrogen atoms bound to the Mn(IV) ion in these Mn(III)Mn(IV) model compounds can be detected easily with ESEEM spectroscopy (*70*−*72*).

The X-ray structures of the dimanganese catalases from *Thermus thermophilis* [at 1 Å (*73*)] and *Lactobacillus plantarum* [at 1.8 Å (*74*)] show that the di-μ_2-oxo-bridged Mn dimer is ligated by two histidine residues, with one histidine ligating each Mn ion. However, ESEEM analyses of the Mn(III)Mn(IV) enzyme conducted at 9−13 GHz detected only one histidyl nitrogen (*75*−*77*). On the basis of the model compound data discussed above, this nitrogen was assigned to the histidine residue that ligates the Mn(IV) ion (*77*). The inability to detect the directly coordinated histidyl nitrogen of the second histidine residue was attributed to either strong or extremely anisotropic hyperfine coupling between this nitrogen and the unpaired electron spin of the Mn(III) ion (*77*), as in the model compounds discussed above.

On the basis of the above considerations, we conclude that, if D1-His170 ligates the $(Mn)_4$ cluster in PSII, detecting the additional nitrogen hyperfine coupling may require either an ESEEM analysis conducted at higher magnetic fields (e.g., 31 GHz) or a pulsed ENDOR analysis. Furthermore, if the additional coupling were to be extremely anisotropic, it would be difficult to detect with either ESEEM or ENDOR. If D1-Asp170 and D1-His170 are eventually shown to ligate the $(Mn)_4$ cluster, analyses of accurate tetrameric exchange coupling models or relevant tetrameric Mn model compounds will be required to determine if the inability to detect the additional nitrogen couplings with an ESEEM analysis conducted at 9.2 GHz provides a clue about the valence of the ligated Mn ion.

One difficulty with proposing that D1-Asp170 ligates the assembled $(Mn)_4$ cluster is the weakly photoautotrophic nature of the D1-D170V mutant and the ability of the D1-D170L and D1-D170I mutants to evolve O_2 (*28*). Neither Val, Leu, nor Ile would be expected to ligate Mn. However, it has been proposed that these residues, being bulky and hydrophobic, cause structural perturbations that permit the D1-Asp170 carboxylate moiety to be replaced with another residue, a peptide carbonyl oxygen, or a water molecule (*28*). As pointed out previously (*28*), compensatory, mutation-induced structural rearrangements have been observed in other systems. In ferredoxin I of *Azotobacter vinelandii*, replacing Cys20 with Ala causes a structural rearrangement that permits the free Cys24 to replace Cys20 as a ligand to the [4Fe-4S] cluster (*78*). In ricin A, replacing active site residue Glu177 with Ala results in the rotation of Glu208 into the active site with partial restoration of catalytic activity (*79*). In human alcohol dehydrogenase, replacing the pyrophosphate-binding residue, Arg47, with Gly results in structural alterations that move Lys228 into the pyrophosphate site with partial restoration of activity (*80*).

Scenario 2. D1-Asp170 Ligates the $(Mn)_4$ Cluster, but D1-His170 Does Not. In this scenario, perhaps for steric reasons, neither nitrogen of the D1-His170 imidazole moiety occupies the same spatial position as the Mn-ligating oxygen of D1-Asp170. Consequently, the Mn-ligating carboxylate oxygen of D1-Asp170 is replaced in the D1-D170H mutant with an oxygen atom from a water molecule or another group. Replacing a coordinating carboxylate oxygen with an oxygen from another moiety would not be expected to change the two-pulse time domain ESEEM spectrum of the S_2 state multiline EPR signal. However, a difficulty with this scenario is that it is difficult to understand why the high-affinity Mn(II) binding site would be retained in the D1-D170H mutant (*23*, *29*), but not in the D1-D170N, D1-D170A, and D1-D170S mutants (*23*, *24*), where the ligating D1-Asp170 carboxylate oxygen could also be replaced with an oxygen atom from a water molecule or other group. One might postulate that D1-His170 separates from the $(Mn)_4$ cluster after the first Mn(II) ion becomes oxidized. The reason might be that Mn(III) and Mn(IV) ions prefer harder Lewis bases as ligands. However, this reasoning does not seem to be compelling because the crystallized dimanganese catalase enzymes discussed above each contain two Mn(III) ions at the active site (*73*, *74*). In these structures, each Mn(III) ion is directly coordinated by a histidyl nitrogen.

Scenario 3. D1-Asp170 Does Not Ligate the Assembled $(Mn)_4$ Cluster. Because D1-Asp170 forms part of the high-affinity binding site of the first Mn(II) ion that is photooxidized during the light-driven assembly of the $(Mn)_4$ cluster (*23*, *24*, *29*), this scenario requires that a structural rearrangement separate D1-Asp170 from the photooxidized Mn(III) ion as the $(Mn)_4$ cluster is formed. We know of no precedent for such a rearrangement in any metalloenzyme except ferritin, where the oxidation of two Fe(II) ions at the binuclear ferroxidase center is followed by transfer of a μ-oxo-bridged Fe(III) dimer to the ferrihydrite core (*81*−*83*). However, in ferritin, the change in the Fe ligation environment is intimately associated with ferritin's function as an iron storage protein. In PSII, there is no apparent need for separating D1-Asp170 from Mn during the assembly of the $(Mn)_4$ cluster.

An additional difficulty with this scenario is explaining why replacing D1-Asp170 with the isosteric residue Asn is far more deleterious to the $(Mn)_4$ cluster's assembly and O_2 evolving activity (*23*, *25*−*27*) than replacing it with the bulky and hydrophobic residues Val, Leu, and Ile (*28*). Whereas D1-D170N cells assemble almost no stable $(Mn)_4$ clusters *in vivo* (*23*, *26*, *27*), D1-D170V cells are weakly photoautotrophic and both D1-D170L and D1-D170I cells evolve O_2 at ∼20% of the rate of wild-type* cells (*28*). One must postulate that Val, Leu, and Ile introduce the same type of structural perturbations that were postulated above for scenario 1. Because D1-Asp170 ligates the first Mn(II) ion that is photooxidized during the light-driven assembly of the $(Mn)_4$ cluster, these structural perturbations must restore the high-affinity Mn(II) binding site sufficiently in D1-D170V, D1-D170L, and D1-D170I cells to permit some $(Mn)_4$ cluster assembly.

A final difficulty is that, if D1-Asp170 merely participates in a hydrogen bond network to the assembled $(Mn)_4$ cluster, one might expect this network to be maintained by Asn. As a precedent, in dihydrofolate reductase, a hydrogen bond network involving Asp27 is retained in the D27N mutant because an O−HN hydrogen bond is simply replaced with an NH−N hydrogen bond (*84*).

CONCLUDING REMARKS

The similarity of the S_1 and S_2 state multiline EPR signals of D1-D170H and wild-type* PSII particles provides further evidence that the assembled $(Mn)_4$ clusters in D1-D170H cells function normally, even though the assembly of the $(Mn)_4$ cluster is inefficient. The similarity of the two-pulse frequency domain ESEEM spectra of the 9.2 GHz S_2 state multiline EPR signals of D1-D170H and wild-type* PSII particles prevents us from concluding definitively whether D1-Asp170 ligates the assembled $(Mn)_4$ cluster. However, if D1-Asp170 ligates the $(Mn)_4$ cluster and the directly coordinating oxygen is replaced with nitrogen in the D1-D170H mutant, the hyperfine coupling between this nitrogen and the unpaired electron spin on the ligated Mn ion must be too strong or anisotropic to be detected in a 9.2 GHz ESEEM analysis. If the coupling is too strong, detecting it will require an ESEEM analysis conducted at a higher magnetic field (e.g., 31 GHz) or require a pulsed ENDOR analysis. If the coupling is extremely anisotropic, it will be difficult to detect with either ESEEM or ENDOR spectroscopy. If D1-Asp 170 is eventually shown to ligate the assembled $(Mn)_4$ cluster, analyses of accurate tetrameric exchange coupling models or relevant tetrameric Mn model compounds may reveal whether our inability to detect additional nitrogen couplings in this study provides a clue about the valence of the ligated Mn ion. Although we favor scenarios involving direct ligation of the $(Mn)_4$ cluster by D1-Asp170, we cannot exclude the possibility that D1-Asp170 ligates only the first Mn(II) ion that is photooxidized during the light-driven assembly of the $(Mn)_4$ cluster, but not the final, assembled $(Mn)_4$ cluster.

ACKNOWLEDGMENT

We are grateful to A. P. Nguyen for maintaining the wild-type* and mutant cultures of *Synechocystis* sp. strain PCC 6803 and for isolating the thylakoid membranes that were used for purifying the PSII particles. We are also grateful to X.-S. Tang for help with the initial phase of this study.

REFERENCES

1. Britt, R. D. (1996) in *Oxygenic Photosynthesis: The Light Reactions* (Ort, D. R., and Yocum, C. F., Eds.) pp 137−164, Kluwer, Dordrecht, The Netherlands.
2. Yachandra, V. K., Sauer, K., and Klein, M. P. (1996) *Chem. Rev. 96*, 2927−2950.
3. Penner-Hahn, J. E. (1998) *Struct. Bonding 90*, 1−36.
4. Debus, R. J. (2000) in *Metal Ions in Biological Systems* (Sigel, A., and Sigel, H., Eds.) Vol. 37, pp 657−711, Marcel Dekker, New York.
5. Tommos, C., and Babcock, G. T. (2000) *Biochim. Biophys. Acta 1458*, 199−219.
6. Pecoraro, V. L., and Hsieh, W.-Y. (2000) in *Metal Ions in Biological Systems* (Sigel, A., and Sigel, H., Eds.) Vol. 37, pp 429−504, Marcel Dekker, New York.
7. Renger, G. (2001) *Biochim. Biophys. Acta 1503*, 210−228.
8. Diner, B. A., and Rappaport, F. (2002) *Annu. Rev. Plant Biol. 53*, 551−580.
9. Vrettos, J. S., and Brudvig, G. W. (2002) *Philos. Trans. R. Soc. London, Ser. B 357*, 1395−1405.
10. Robblee, J. H., Cinco, R. M., and Yachandra, V. K. (2001) *Biochim. Biophys. Acta 1503*, 7−23.
11. Dau, H., Iuzzolino, L., and Dittmer, J. (2001) *Biochim. Biophys. Acta 1503*, 24−39.
12. Yachandra, V. K. (2002) *Philos. Trans. R. Soc. London, Ser. B 357*, 1347−1358.
13. Zheng, M., and Dismukes, G. C. (1996) *Inorg. Chem. 35*, 3307−3319.
14. Carrell, T. G., Tyryshkin, A. M., and Dismukes, G. C. (2002) *J. Biol. Inorg. Chem. 7*, 2−22.
15. Messinger, J., Robblee, J. H., Bergmann, U., Fernandez, C., Glatzel, P., Visser, H., Cinco, R. M., McFarlane, K. L., Bellacchio, E., Pizarro, S. A., Cramer, S. P., Sauer, K., Klein, M. P., and Yachandra, V. K. (2001) *J. Am. Chem. Soc. 123*, 7804−7820.
16. Zouni, A., Witt, H. T., Kern, J., Fromme, P., Krauss, N., Saenger, W., and Orth, P. (2001) *Nature 409*, 739−743.
17. Fromme, P., Kern, J., Loll, B., Biesiadka, J., Saenger, W., Witt, H. T., Krauss, N., and Zouni, A. (2002) *Philos. Trans. R. Soc. London, Ser. B 357*, 1337−1345.
18. Kamiya, N., and Shen, J.-R. (2003) *Proc. Natl. Acad. Sci. U.S.A. 100*, 98−103.
19. Peloquin, J. M., Campbell, K. A., Randall, D. W., Evanchik, M. A., Pecoraro, V. L., Armstrong, W. H., and Britt, R. D. (2000) *J. Am. Chem. Soc. 122*, 10926−10942.
20. Peloquin, J. M., and Britt, R. D. (2001) *Biochim. Biophys. Acta 1503*, 96−111.
21. Diner, B. A. (2001) *Biochim. Biophys. Acta 1503*, 147−163.
22. Debus, R. J. (2001) *Biochim. Biophys. Acta 1503*, 164−186.
23. Nixon, P. J., and Diner, B. A. (1992) *Biochemistry 31*, 942−948.
24. Diner, B. A., and Nixon, P. J. (1992) *Biochim. Biophys. Acta 1101*, 134−138.
25. Boerner, R. J., Nguyen, A. P., Barry, B. A., and Debus, R. J. (1992) *Biochemistry 31*, 6660−6672.
26. Chu, H.-A., Nguyen, A. P., and Debus, R. J. (1994) *Biochemistry 33*, 6137−6149.
27. Whitelegge, J. P., Koo, D., Diner, B. A., Domian, I., and Erickson, J. M. (1995) *J. Biol. Chem. 270*, 225−235.
28. Chu, H.-A., Nguyen, A. P., and Debus, R. J. (1995) *Biochemistry 34*, 5839−5858.
29. Campbell, K. A., Force, D. A., Nixon, P. J., Dole, F., Diner, B. A., and Britt, R. D. (2000) *J. Am. Chem. Soc. 122*, 3754−3761.
30. Chu, H.-A., Debus, R. J., and Babcock, G. T. (2001) *Biochemistry 40*, 2312−2316.
31. Kevan, L. (1990) in *Modern Pulsed and Continuous-Wave Electron Spin Resonance* (Kevan, L., and Bowman, M. K., Eds.) pp 231−266, Wiley-Interscience, New York.
32. Dikanov, S. A., and Tsvetkov, Y. D. (1992) *Electron Spin-Echo Envelope Modulation (ESEEM) Spectroscopy*, CRC Press, Boca Raton, FL.
33. Britt, R. D. (1996) in *Biophysical Techniques in Photosynthesis* (Amesz, J., and Hoff, A. J., Eds.) pp 235−253, Kluwer, Dordrecht, The Netherlands.
34. Chasteen, N. D., and Snetsinger, P. A. (2000) in *Physical Methods in Bioinorganic Chemistry: Spectroscopy and Magnetism* (Que, L., Jr., Ed.) pp 187−231, University Science Books, Sausalito, CA.
35. Deligiannakis, Y., Louloudi, M., and Hadjiliadis, N. (2000) *Coord. Chem. Rev. 204*, 1−112.
36. Debus, R. J., Campbell, K. A., Gregor, W., Li, Z.-L., Burnap, R. L., and Britt, R. D. (2001) *Biochemistry 40*, 3690−3699.
37. Debus, R. J., Nguyen, A. P., and Conway, A. B. (1990) in *Current Research in Photosynthesis* (Baltscheffsky, M., Ed.) Vol. I, pp 829−832, Kluwer, Dordrecht, The Netherlands.
38. Rippka, R., Deruelles, J., Waterbury, J. B., Herdman, M., and Stanier, R. Y. (1979) *J. Gen. Microbiol. 111*, 1−61.
39. Hays, A.-M. A., Vassiliev, I. R., Golbeck, J. H., and Debus, R. J. (1998) *Biochemistry 37*, 11352−11365.
40. Debus, R. J., Campbell, K. A., Peloquin, J. M., Pham, D. P., and Britt, R. D. (2000) *Biochemistry 39*, 470−478.
41. Sturgeon, B. E., and Britt, R. D. (1992) *Rev. Sci. Instrum. 63*, 2187−2192.
42. Campbell, K. A., Peloquin, J. M., Pham, D. P., Debus, R. J., and Britt, R. D. (1998) *J. Am. Chem. Soc. 120*, 447−448.
43. Campbell, K. A., Gregor, W., Pham, D. P., Peloquin, J. M., Debus, R. J., and Britt, R. D. (1998) *Biochemistry 37*, 5039−5045.

44. Debus, R. J., Campbell, K. A., Pham, D. P., Hays, A.-M. A., and Britt, R. D. (2000) *Biochemistry 39*, 6275−6287.
45. Mims, W. B. (1984) *J. Magn. Reson. 59*, 291−306.
46. Tang, X.-S., and Diner, B. A. (1994) *Biochemistry 33*, 4594−4603.
47. Gilchrist, M. L., Jr. (1996) Ph.D. Dissertation, University of California, Davis, CA.
48. Stewart, D. H., and Brudvig, G. W. (1998) *Biochim. Biophys. Acta 1367*, 63−87.
49. Tang, X.-S., Diner, B. A., Larsen, B. S., Gilchrist, M. L., Jr., Lorigan, G. A., and Britt, R. D. (1994) *Proc. Natl. Acad. Sci. U.S.A. 91*, 704−708.
50. Britt, R. D., Zimmermann, J.-L., Sauer, K., and Klein, M. P. (1989) *J. Am. Chem. Soc. 111*, 3522−3532.
51. Mims, W. B. (1972) *Phys. Rev. B 5*, 2409−2419.
52. Mims, W. B. (1972) *Phys. Rev. B 6*, 3543−3545.
53. Mims, W. B., and Peisach, J. (1989) in *Advanced EPR: Applications in Biology and Biochemistry* (Hoff, A. J., Ed.) pp 1−57, Elsevier, Amsterdam.
54. DeRose, V. J., Yachandra, V. K., McDermott, A. E., Britt, R. D., Sauer, K., and Klein, M. P. (1991) *Biochemistry 30*, 1335−1341.
55. Boussac, A., Deligiannakis, Y., and Rutherford, A. W. (1998) in *Photosynthesis: Mechanisms and Effects* (Garab, G., Ed.) Vol. II, pp 1233−1240, Kluwer, Dordrecht, The Netherlands.
56. Van Camp, H. L., Sands, R. H., and Fee, J. A. (1981) *J. Chem. Phys. 75*, 2098−2107.
57. Yokoi, H. (1982) *Biochem. Biophys. Res. Commun. 108*, 1278−1284.
58. Hüttermann, J., and Kappl, R. (1987) in *Metal Ions in Biological Systems* (Sigel, H., Ed.) Vol. 22, pp 1−80, Marcel Dekker, New York.
59. Mims, W. B., and Peisach, J. (1978) *J. Chem. Phys. 69*, 4921−4930.
60. Mims, W. B., and Peisach, J. (1979) *J. Biol. Chem. 254*, 4321−4323.
61. Jiang, F., McCracken, J., and Peisach, J. (1990) *J. Am. Chem. Soc. 112*, 9035−9044.
62. McCracken, J., Peisach, J., and Dooley, D. M. (1987) *J. Am. Chem. Soc. 109*, 4064−4072.
63. McCracken, J., Pember, S., Benkovic, S. J., Villafranca, J. E., Miller, R. J., and Peisach, J. (1988) *J. Am. Chem. Soc. 110*, 1069−1074.
64. McCracken, J., Peisach, J., Bhattacharyya, L., and Brewer, F. (1991) *Biochemistry 30*, 4486−4491.
65. Espe, M. P., Hosler, J. P., Ferguson-Miller, S., Babcock, G. T., and McCracken, J. (1995) *Biochemistry 34*, 7593−7602.
66. Lee, H. C., Goroncy, A. K., Peisach, J., Cavada, B. S., Grangeiro, T. B., Ramos, M. V., Sampaio, A. H., Dam, T. K., and Brewer, C. F. (2000) *Biochemistry 39*, 2340−2346.
67. Robblee, J. H., Messinger, J., Cinco, R. M., McFarlane, K. L., Fernandez, C., Pizarro, S. A., Sauer, K., and Yachandra, V. K. (2002) *J. Am. Chem. Soc. 124*, 7459−7471.
68. Tan, X.-L., Gultneh, Y., Sarneski, J. E., and Scholes, C. P. (1991) *J. Am. Chem. Soc. 113*, 7853−7858.
69. Khangulov, S., Sivaraja, M., Barynin, V. V., and Dismukes, G. C. (1993) *Biochemistry 32*, 4912−4924.
70. Randall, D. W. (1997) Ph.D. Dissertation, University of California, Davis, CA.
71. Britt, R. D., and Klein, M. P. (1992) in *Pulsed Magnetic Resonance: NMR, ESR, and Optics, a Recognition of E. L. Hahn* (Bagguley, D. M. S., Ed.) pp 361−376, Clarendon Press, Oxford, U.K.
72. Sturgeon, B. E. (1994) Ph.D. Dissertation, University of California, Davis, CA.
73. Antonyuk, S. V., Melik-Adamyan, V. R., Popov, A. N., Lamzin, V. S., Hempstead, P. D., Harrison, P. M., Artymyuk, P. J., and Barynin, V. V. (2000) *Kristallografiya 45*, 111−122; *Crystallogr. Rep. (Transl. Kristallografiya) 45*, 105−116.
74. Barynin, V. V., Whittaker, M. M., Antonyuk, S. V., Lamzin, V. S., Harrison, P. M., Artymiuk, P. J., and Whittaker, J. W. (2001) *Structure 9*, 725−738.
75. Dikanov, S. A., Tsvetkov, D., Kangulov, S. V., and Gol′dfel′d, M. G. (1988) *Dokl. Akad. Nauk SSSR 302*, 1255−1257; *Dokl. Biophys. (Transl. of Dokl. Akad. Nauk) 302* 174−177.
76. Ivancich, A., Barynin, V. V., and Zimmermann, J.-L. (1995) *Biochemistry 34*, 6628−6639.
77. Stemmler, T. L., Sturgeon, B. E., Randall, D. W., Britt, R. D., and Penner-Hahn, J. E. (1997) *J. Am. Chem. Soc. 119*, 9215−9225.
78. Martín, A. E., Burgess, B. K., Stout, C. D., Cash, V. L., Dean, D. R., Jensen, G. M., and Stephens, P. M. (1990) *Proc. Natl. Acad. Sci. U.S.A. 87*, 598−602.
79. Kim, Y., Misna, D., Monzingo, A. F., Ready, M. P., Frankel, A., and Robertus, J. D. (1992) *Biochemistry 31*, 3294−3296.
80. Stone, C. L., Hurley, T. D., Amzel, L. M., Dunn, M. F., and Bosron, W. F. (1993) in *Enzymology and Molecular Biology of Carbonyl Metabolism 4* (Weiner, H., Ed.) pp 429−437, Plenum Press, New York.
81. Harrison, P. M., and Arosio, P. (1996) *Biochim. Biophys. Acta 1275*, 161−203.
82. Chasteen, N. D., and Harrison, P. M. (1999) *J. Struct. Biol. 126*, 194.
83. Theil, E. C. (2000) in *Handbook of Metalloproteins* (Messerschmidt, A., Huber, R., Poulos, T. L., and Wieghardt, K., Eds.) pp 771−781, Wiley, Chichester, U.K.
84. Howell, E. E., Villafranca, J. E., Warren, M. S., Oatley, S. J., and Kraut, J. (1986) *Science 231*, 1123−1128.

BI034859F